Effects of electric field on confined electrolyte in a hexagonal mesoporous silica

Weiyi Lu,[1] Taewan Kim,[2] Aijie Han,[3] Xi Chen,[4] and Yu Qiao[1,2,a)]
[1]*Department of Structural Engineering, University of California – San Diego, La Jolla, California 92093-0085, USA*
[2]*Program of Materials Science & Engineering, University of California – San Diego, La Jolla, California 92093, USA*
[3]*Department of Chemistry, University of Texas – Pan American, Edinburg, Texas 78539, USA*
[4]*Department of Earth & Environmental Engineering, Columbia University, New York, New York 10027, USA*

(Received 16 February 2011; accepted 6 May 2011; published online 26 May 2011)

In an electrowetting experiment on a surface treated hexagonal mesoporous silica, it is noticed that the effective solid-liquid interfacial tension is quite insensitive to the applied voltage, while the accessible nanopore volume decreases significantly as the voltage is increased. When the voltage is higher than 900 V, the liquid infiltration cannot be detected. The liquid defiltration is quite insensitive to the electric field. These unique phenomena may be attributed to the field responsive ion behaviors in the confining nanoenvironment. © *2011 American Institute of Physics*. [doi:10.1063/1.3594791]

I. INTRODUCTION

While nanofluidic behaviors have been studied intensively through both experiments and computer simulations for more than a decade, many of their properties are still quite inadequately understood. First, the molecular structures are highly dependent on the confining nanoenvironment. If the nanotube/nanopore radius, r, is close to the molecular size, the confined water molecules would form a quasi-one-dimensional chain.[1,2] If a high external pressure is applied, a double helical structure may be observed, which has a higher system free energy but a lower column resistance per unit surface area.[3] As the nanochannel size increases, across the cross section there can be a few layers of water molecules.[4] The effective molecular density and the characteristic length scale are related to not only the nanochannel geometry, but also the solid and liquid properties, which often need to be redefined at the nanometer scale.[5,6]

If there are solvated ions in the liquid, at the opening and the interior of a nanochannel, the solvated ions can be regarded as a heterogeneous phase.[7] The infiltration of ions into a nominally wettable nanochannel may be difficult, if there is no sufficient space for the required "free volume."[8,9] The preferences of entrance of cations and anions are quite different, which significantly affects the configuration of the confined ions.[10] Inside a molecular-sized nanopore, the hydration shell surrounding an ion cannot be developed, and, thus, the solvated structure would be reduced to a chain of crystalline-like ion couples. The distance between the adjacent ion couples dominates the system free energy, which in turn determines the effective flow rate, the required input energy, as well as the sustainability of continuous infiltration.[11] If the nanochannel size is larger than but comparable with the size of the hydration shell, the hydration shell can be developed but is considerably distorted along the axial direction, exhibiting configurations of less coordination numbers and higher energies.[12,13] The confined ions would influence the layered structure of water molecules, with a nonlinear relationship with the nanochannel size.[14] In a relatively large nanochannel, the solvated structure can be similar with that in bulk phase, while the solvated ions would interact with the confined water, due to the anisotropy of the environment, the different behaviors of cations and anions, etc.[15–17]

If the nanochannel inner surface is initially unaccessible, the system free energy change associated with the liquid infiltration can be assessed by measuring the required external energy that triggers the formation of confined liquid phase. If the nanochannel or nanotube length is short, the liquid molecules can transport across it in a "frictionless" manner, with the aid of thermal energy.[18] In a long nanochannel, the slip boundary condition of liquid molecules along the solid wall can be related to the "shear resistance."[19]

The nanofluidic behaviors can be field responsive. As temperature varies, the effective solid-liquid interfacial tension can change considerably,[20,21] so does the confined molecular and ionic configuration.[22] Another vital factor is the electric potential, especially when the liquid is effectively conductive. It is envisioned that, if the solid-liquid interfacial energy is controlled by applying a voltage, as this effect is greatly amplified by the high specific surface area of nanochannels, the system can be of great applicability for active control, energy conversion and storage, selective absorption and adsorption, smart catalysis, etc.[23] For instance, under a dynamic loading if liquid can be intruded into nanopores, the energy that the confined liquid phase carries can be regarded as being "captured," since (1) the energy transmission across the thin nanopore wall, which can be effectively incompressible if the nanopore wall is formed by a single or only a few atomic layers, is difficult, and/or (2) in a nanoporous material the confined gas and/or liquid phases and the nanopore walls form a highly heterogeneous structure

a)Author to whom correspondence should be addressed. Electronic mail: yqiao@ucsd.edu. Telephone: 858-534-3388. Fax: 858-822-2260.

of large impedance mismatch between adjacent components, through which little stress wave energy can transmit. If the liquid infiltration behaviors can be controlled electrically, interactive protection systems can be developed based on this energy capture mechanism. However, currently, not only the fundamental theories but also many important experimental observations are still lacking. The current study will be focused on the electric field effects on the behaviors of confined liquids in a hexagonal mesoporous silica (HMS), discussed below.

II. EXPERIMENTAL

The HMS sample was obtained from Sigma-Aldrich, with the particle size around 2–8 μm. Compared with many other silica gels, the HMS is of a relatively regular porous structure and a high surface area. By using a Micromeritics Tristar-3000 Analyzer, the average nanopore size was measured to be 3.5 nm. The raw material was hydrophilic. In order to directly measure the system free energy change associated with the liquid infiltration, the nanopore inner surfaces were first dehydrated in vacuum at 120 °C for 12 h. With the moisture content being kept low by a drying tube, in a round-bottom flask the material was mixed with 2.5% of chlorotrimethylsilane in dry toluene. The mixture was refluxed at 90 °C for 48 h, and then repeatedly rinsed in dry toluene, methanol, and distilled water. The treated HMS particles were compressed under 15 MPa to form thin disks. The disk thickness was 0.2 mm and the diameter was 12.7 mm. Through a gas absorption analysis it was confirmed that since the peak pressure was relatively low, the nanoporous structure was not affected by the compression process.

A 120 μm thick gold film was employed as the electrode. The gold film was coated by a 50 μm thick teflon layer, and folded repeatedly into a layer stack, as depicted in Fig. 1. The layer stack consisted of 12 identical layers. In between adjacent layers, HMS disks were placed. The HMS-gold layer stack was firmly compressed so that the HMS phase and the gold electrode fully contacted with each other. The HMS-gold layer stack was covered by another teflon coated gold film (the counter electrode), separated by a porous polypropylene membrane. The polypropylene membrane was 100 μm thick.

The system was immersed in saturated lithium chloride solution in a stainless steel cylinder. The cylinder was sealed by two stainless steel pistons from the top and the bottom, respectively. An external voltage was applied across the electrode and the counter electrode by a Proteck type 6030 DC power supply. The applied voltage, ϕ, was in the range of 360 V to 900 V.

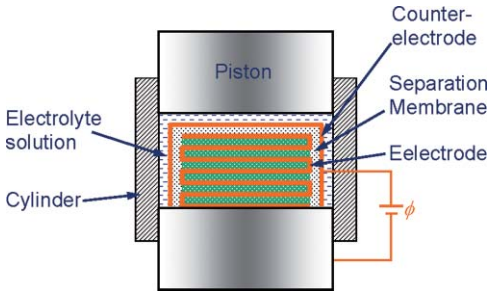

FIG. 1. Schematic of the experimental setup.

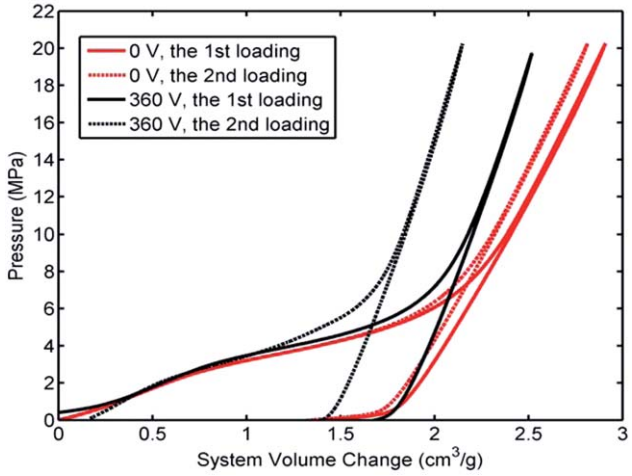

FIG. 2. Typical sorption isotherm curves when the applied voltage is 360 V.

When a constant voltage was maintained, the upper piston was intruded into the cylinder by a type 5580 Instron machine at a loading rate of 1 mm/min. By measuring the piston displacement, the system volume change could be calculated. The quasi-hydrostatic pressure in the liquid phase was taken as the piston pressure. When the pressure was increased to about 20 MPa, the piston was moved out of the cylinder at the same rate of 1 mm/min. After the first loading-unloading cycle, similar procedure was repeated for 2–3 times. From the second loading, the measured testing curves in the following loading cycles were nearly identical, and, therefore, the following discussion will be focused on the first two loading-unloading cycles. Figures 2–5 show typical sorption isotherm curves.

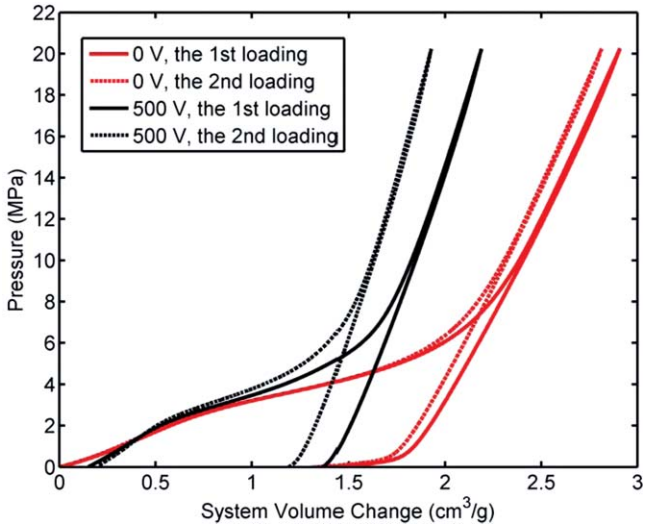

FIG. 3. Typical sorption isotherm curves when the applied voltage is 500 V.

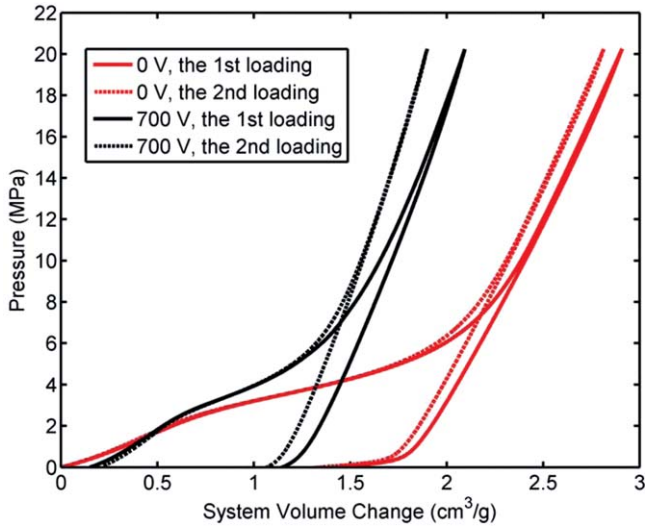

FIG. 4. Typical sorption isotherm curves when the applied voltage is 700 V.

III. RESULTS AND DISCUSSION

After the surface treatment, the nanopore inner surfaces are grafted by a monolayer of silyl groups.[24] The addition of the electrolyte in the liquid phase not only improves the electric conductivity, but also modifies the surface and interfacial tensions, so that the effective degree of hydrophobicity further increases.[25–27] Without an external pressure, the liquid phase cannot enter the nanopores. As the pressure increases, the system volume decreases quite linearly, as the empty HMS particles are compressed and close-packed. When the pressure reaches about 2.5 MPa, the energy barrier of the nanopore inner surfaces is overcome, and the liquid starts to infiltrate into the nanopores. As a result, an infiltration plateau is formed. The pressure rises as the liquid enters smaller nanopores, until the nanoporous space is fully occupied. After the pressure is increased to about 9.5 MPa, the infiltration is completed. Without any external electric field, the width of infiltration plateau, which is defined as the distance between the low-pressure and high-pressure linear sections, is about 1.3 cm^3/g, close to the measured specific nanopore volume. The onset of infiltration is taken as the point where the slope of sorption isotherm curve decreases by 50% from the slope of the low-pressure linear section.

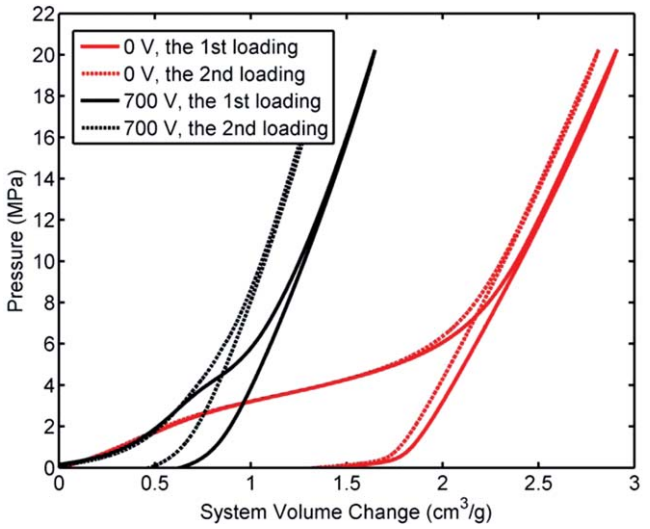

FIG. 5. Typical sorption isotherm curves when the applied voltage is 900 V.

As the loading-unloading process is repeated, the major characteristics of the infiltration-defiltration cycle remain the same, except that the infiltration volume is slightly smaller. Clearly, during the unloading process of the first cycle, most of the confined liquid defiltrates out of the nanopores, and the nanoporous space is available for the second infiltration. The slight reduction in infiltration volume at the second loading may be related to the defects in nanoporous structure and/or the largest nanopores, where the formation and expansion of gas/vapor nanophase are difficult.[28,29] The defiltration happens at a much lower pressure compared with the infiltration, which may be attributed to the energy barrier of nanopore walls to the confined liquid motion, the mass and energy exchanges among gas/vapor and liquid phases, and the surface diffusion effect,[29–33] which is still an active topic of fundamental research.

As a high voltage is applied, a relatively strong electric field is created across the electrode-liquid interface through the HMS layer. The teflon coating insulates the liquid from the electrode, so that no electrochemical reactions would take place. The electric field would considerably change the surface ion configuration. At a large solid surface, according to the classic electrowetting theory, the solid-liquid interfacial tension decreases as the applied voltage increases. The effect of the direction of electric field is secondary.[34]

In a nanopore, because across the cross section there are only a limited number of ions and water molecules, continuum concepts, e.g., the definitions of contact angle and surface tension, are no longer valid. Therefore, the following discussion will be focused on the system free energy variation. If the ion behaviors in the liquid phase confined in the HMS nanopores were similar with that in bulk phase, the infiltration pressure, P, which can be related to the system free energy change ($\Delta\gamma$) by $P = 2 \cdot \Delta\gamma/r$, should be reduced. Here, $\Delta\gamma$ is defined as the system free energy increase as a unit area of nanopore inner surface is exposed to the confined liquid phase. Note that the infiltration volume should not vary, since the nanoporous structure, particularly the nanopore volume, is not dependent on the electric field.

From Fig. 2, it can be seen that when $\phi = 360$ V, the infiltration pressure does not vary much, while the infiltration volume decreases, which is contradictory to the above discussion of classic electrowetting theory. If the infiltration pressure is constant, $\Delta\gamma$ is also constant, which is against the literature data of high-salinity electrolyte solutions.[35] Because the nanoporous structure is not related to the external electric field, as long as the external pressure is sufficiently high, the nanopores should be filled. The measured reduction in infiltration volume shows that a portion of the nanopores becomes unaccessible after the voltage is applied.

At the second loading, both the infiltration pressure and the infiltration volume decrease, somewhat similar with the

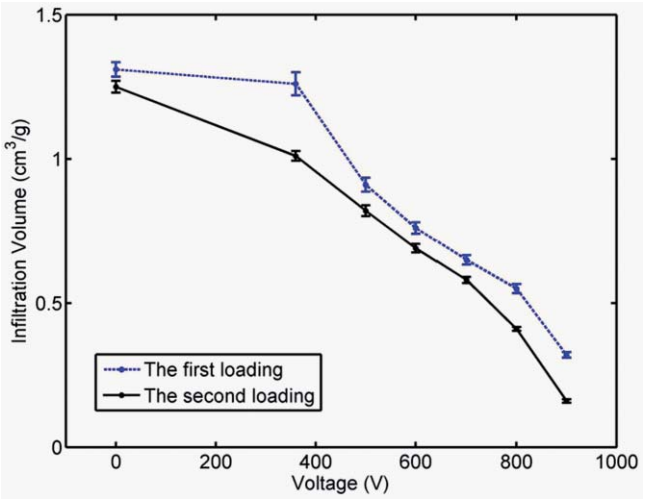

FIG. 6. The infiltration volume as a function of the applied voltage.

uncharged system, suggesting that the defiltration behaviors of confined liquid are relatively insensitive to ϕ.

The effects of voltage become more pronounced as ϕ becomes higher. From Figs. 2–5, it can be seen that when ϕ is 360 V, 500 V, 700 V, and 900 V, the infiltration volumes at the first loading are 1.26 cm^3/g, 0.9 cm^3/g, 0.65 cm^3/g, and 0.32 cm^3/g, respectively; the infiltration volumes at the second loading are typically 0.05–0.1 cm^3/g smaller. The infiltration pressure varies quite randomly as the voltage changes.

These phenomena are shown more clearly in Figs. 6 and 7. For self-comparison purpose, the infiltration pressure is taken as the pressure at the middle point of the infiltration plateau in sorption isotherm curve. There are no clear patterns of the relationship between the infiltration pressure and the voltage. The slight change in so-defined infiltration pressure is associated with the variation in infiltration volume, and may not reflect the difference in system free energy variation. In the voltage range of 360 V to 900 V, at both the first and the second loadings, the infiltration volume decreases quite linearly as ϕ rises. The difference between the infiltration volumes of the two loadings is nearly constant, which may be

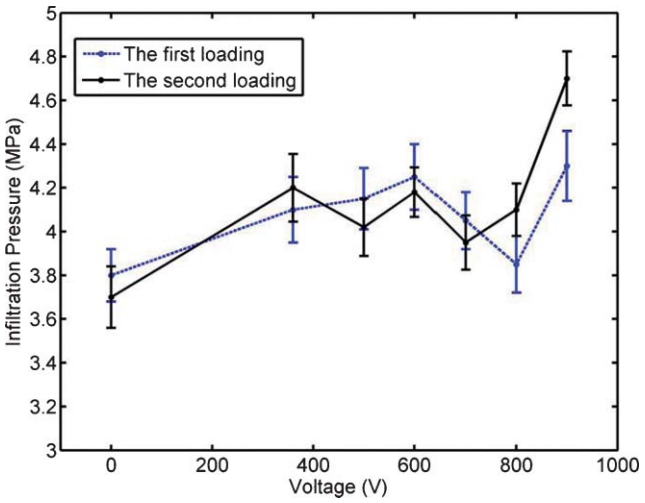

FIG. 7. The infiltration pressure as a function of the applied voltage.

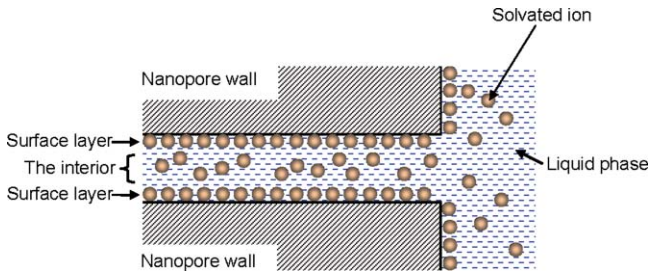

FIG. 8. Schematic of confined ions in a nanopore.

related to the intrinsic defects in nanoporous structure that is independent of the environmental factors.

These unique phenomena may be related to the confined ion structures, as depicted in Fig. 8. The nanopore size of the HMS under investigation ranges from 2–10 nm. In such small nanopores, especially in the smallest nanopores, the hydration shell of a solvated ion may not be fully developed. More importantly, the ion distribution is highly confined along the radius direction.

In a relatively large nanopore, similar with the electrowetting effect at a large solid surface, the like charged ions are repelled. The overall confined liquid must be charge-balanced. The ion repelling occurs along the radius direction. As an ion concentration difference is built up between the surface layer and the interior, the ion diffusion may take place along the axial direction, so that the osmotic pressure is minimized. However, the axial ion motion may not immediately affect the system free energy.

In a relatively small nanopore, most of the ions are directly exposed to the nanopore inner surface; that is, in the interior of the nanopore there is no a bulk phase that acts as an ion reservoir. With the external electric field, along the radius direction, due to the small length scale, the potential gradient cannot be developed, and, thus, the ion distribution is quite insensitive to the voltage variation. Under this condition, the mass and energy exchange between the confined liquid phase and the bulk liquid phase outside is suppressed.

Because of the nanopore size effect on the potential dependence of the effective ion density of confined liquid, when the electric field is relatively low, only the confined liquid in the largest nanopores is affected. When the ion structure reaches the equilibrium condition, the system free energy variation is much reduced, and the nanopore inner surface may be effectively wettable. Under ambient condition, these nanopores can be soaked up by the liquid phase spontaneously, and in the following loading-unloading process they are not involved in the infiltration of pressurized liquid, leading to the reduction in measured infiltration volume. In the relatively small nanopores, the voltage effect on the ion structure is relatively mild. While the absolute value of system free energy variation may slightly decrease, due to the decrease in the average size of the nanopores accessible to the pressurized liquid, the relationship between the infiltration pressure and the magnitude of voltage is quite nonlinear.

With the increasing voltage, the electric field effects are more pronounced in smaller nanopores. As more and more nanopore surfaces are effectively wettable, the nanopore

volume associated with the pressure induced infiltration decreases. The testing data show that when $\phi > 900$ V, the infiltration plateau nearly vanishes, suggesting that the suppression effect saturates.

As the external pressure is lowered during the unloading process, the molecular and ionic transport is more dominated by the surface diffusion processes. As long as the confined liquid phase is formed and the nanopores are well connected, the liquid should come out of the energetically unfavorable nanoenvironment. This process is less dependent on the applied voltage.

IV. CONCLUSION

In a relatively large nanopore and a relatively small nanopore, the effects of external electric field on the motion of confined liquid are different. When the nanopore size is relatively large, the electric field effect can be predicted by the classic electrowetting theory. When the voltage increases, the system free energy variation associated with liquid infiltration decreases. When the nanopore size is relatively small, due to the lack of ion reservoir in the interior, the electric field effect is suppressed. As a result, in the pressure induced infiltration experiment, the measured infiltration volume is reduced significantly as the applied voltage increases, and the infiltration pressure varies somewhat randomly. The defiltration of confined liquid is less affected by the external electric field.

ACKNOWLEDGMENTS

This work was supported by the National Science Foundation (NSF) under Grant No. ECCS-1028010.

[1] Y. Qiao, L. Liu, and X. Chen, Nano Lett. **9**, 984 (2009).
[2] X. Chen, G. Cao, A. Han, V. K. Punyamurtula, L. Liu, P. J. Culligan, T. Kim, and Y. Qiao, Nano Lett. **8**, 2988 (2008).
[3] B. Y. Cao, J. Sun, M. Chen, and Z. Y. Guo, Int. J. Mol. Sci. **10**, 4638 (2009).
[4] D. Mattia and Y. Gogotsi, Microfluid. Nanofluid. **5**, 289 (2008).
[5] A. Han and Y. Qiao, J. Mater. Res. **24**, 2416 (2009).
[6] A. Han and Y. Qiao, Chem. Phys. Lett. **454**, 294 (2008).
[7] J. Zhao, P. J. Culligan, Y. Qiao, Q. Zhou, Y. Li, M. Tak, T. Park, and X. Chen, J. Phys.: Condens. Matter **22**, 315301 (2010).
[8] A. Han and Y. Qiao, J. Am. Chem. Soc. **128**, 10348 (2006).
[9] D. T. Wasan and A. D. Nikolov, Nature (London) **423**, 156 (2003).
[10] T. Kim, W. Lu, A. Han, V. K. Punyamurtula, X. Chen, and Y. Qiao, Appl. Phys. Lett. **94**, 013105 (2009).
[11] L. Liu, X. Chen, W. Lu, A. Han, and Y. Qiao, Phys. Rev. Lett. **102**, 184501 (2009).
[12] D. Li and H. T. Wang, J. Mater. Chem. **20**, 4551 (2010).
[13] V. Sridhara, B. S. Gowrishankar, C. Snehalatha, and L. N. Satapathy, Trans. Indian Ceram. Soc. **68**, 1 (2009).
[14] L. Bocquet and E. Charlaix, Chem. Soc. Reviews **39**, 1073 (2010).
[15] W. Sparreboom, A. Van Den Berg, and J. C. T. Eijkel, New J. Physics **12**, 15004 (2010).
[16] J. C. T. Eijkel and A. Van Den Berg, Chem. Soc. Rev. **39**, 957 (2010).
[17] W. Lu, A. Han, T. Kim, V. K. Punyamurtula, X. Chen, and Y. Qiao, Appl. Phys. Lett. **94**, 023106 (2009).
[18] B. J. Hinds, N. Chopra, T. Rantell, R. Andrews, V. Gavalas, and L. G. Bachas, Science **303**, 62 (2004).
[19] G. Cao, Y. Qiao, Q. Zhou, and X. Chen, Philos. Mag. Lett. **88**, 371 (2008).
[20] A. Han and Y. Qiao, Phil. Mag. Lett. **87**, 25 (2007).
[21] F. B. Surani, A. Han, and Y. Qiao, J. Mater. Res. **21**, 2389 (2006).
[22] L. Liu, J. B. Zhao, P. J. Culligan, Y. Qiao, and X. Chen, Langmuir **25**, 11862 (2009).
[23] W. Lu, T. Kim, A. Han, X. Chen, and Y. Qiao, Langmuir **25**, 9463 (2009).
[24] A. Han and Y. Qiao, Chem. Lett. **36**, 882 (2007).
[25] A. Han and Y. Qiao, J. Mater. Res. **22**, 644 (2007).
[26] L. J. Cheng and L. J. Guo, Chem. Soc. Rev. **39**, 923 (2010).
[27] M. Z. Bazant, M. S. Kilic, B. D. Storey, and A. Ajdari, Adv. Colloid Interface Sci. **152**, 48 (2009).
[28] J. M. Reese and Y. H. Zhang, J. Comput. Theo. Nanosci. **6**, 2061 (2009).
[29] A. Han, X. Kong, and Y. Qiao, J. Appl. Phys. **100**, 014308 (2006).
[30] A. Han and Y. Qiao, J. Phys. D: Appl. Phys. **40**, 3436 (2007).
[31] A. Han, W. Lu, V. K. Punyamurtula, T. Kim, and Y. Qiao, J. Appl. Phys. **105**, 024309 (2009).
[32] X. Kong and Y. Qiao, Appl. Phys. Lett. **86**, 151919 (2005).
[33] F. B. Surani and Y. Qiao, J. Appl. Phys. **100**, 034311 (2006).
[34] C. N. Baroud, F. Gallaire, and R. Dangla, Lab Chip **10**, 2032 (2010).
[35] W. Freyland, Phys. Chem. Chem. Phys. **10**, 923 (2008).